This is a preprint of the following article:
B. J. Brelje and J. R. R. A. Martins. Development of a Conceptual Design Model for Aircraft Electric Propulsion with Efficient Gradients. *Electric Aircraft Technologies Symposium*, 2018.
The published article may differ from this preprint. Copyright 2018 Benjamin J. Brelje and Joaquim R.R.A Martins, All Rights Reserved

Development of a Conceptual Design Model for Aircraft Electric Propulsion with Efficient Gradients

Benjamin J. Brelje*† and Joaquim R.R.A. Martins‡
University of Michigan, Ann Arbor, Michigan

Research on electric aircraft propulsion has greatly expanded in the last decade, revealing new insights on the unique features of the electric aircraft design problem, and identifying shortcomings in existing analysis techniques and tools. In this paper, we survey currently-available analysis codes for aircraft with electric propulsion. We introduce a new conceptual design and optimization toolkit—OpenConcept—built for aircraft incorporating electric propulsion. OpenConcept consists of three parts: a library of simple, conceptual-level models of common electric propulsion components; a set of analysis routines necessary for aircraft sizing and optimization; and several example aircraft models. All of OpenConcept's codes have been analytically differentiated, enabling the use of OpenMDAO 2's efficient Newton solver, as well as gradient-based optimization methods. OpenConcept supports parametric cost modeling and waste heat management at the component level, enabling realistic thermal and economic constraints in optimization studies. We present a case study involving the electrification of existing turboprop airplanes. We model the Daher TBM 850 and Beechcraft King Air C90GT in OpenConcept, and validate the sizing, weights, fuel burn, and takeoff field length analyses. We then define a series hybrid electric propulsion architecture for the King Air, and perform a retrofit study. Finally, we perform multidisciplinary design optimization to minimize both fuel burn and trip cost for varying design ranges and assumed battery specific energy levels. We ran more than 750 multidisciplinary optimization cases with full mission analysis. Each optimization runs in approximately 2 minutes on a typical notebook PC. We demonstrate that OpenConcept is a flexible and efficient way of performing conceptual-level analysis of aircraft with unconventional propulsion architectures.

Nomenclature

η	=	efficiency
γ	=	flight path angle
μ	=	tire rolling or braking friction coefficient
a	=	acceleration
BFL	=	balanced field length
c	=	cost
C_{D_0}	=	zero-lift drag coefficient
C_L	=	lift coefficient
C_P	=	propeller power coefficient
D	=	drag force
d_{prop}	=	propeller diameter

*PhD Candidate, Department of Aerospace Engineering, AIAA Student Member
†The author is also an employee of The Boeing Company; this article is written in a personal capacity.
‡Professor, Department of Aerospace Engineering, AIAA Associate Fellow

$e_{(b)}$	=	(battery) specific energy (energy / mass)
E	=	energy
EASA	=	European Aviation Safety Agency
EP	=	electric propulsion
FAA	=	Federal Aviation Administration
g	=	gravitational acceleration
H_E	=	degree of hybridization with respect to energy (percentage of mission energy from electricity)
h_o	=	takeoff obstacle clearance height
ISA	=	International Standard Atmosphere
J	=	propeller advance ratio
KIAS	=	knots indicated airspeed
L	=	lift force
m	=	mass
MDO	=	multidisciplinary design optimization
MLW	=	maximum landing weight
MTOW	=	maximum takeoff weight
OEI	=	one engine inoperative
OEM	=	(aircraft) original equipment manufacturer
p	=	specific power (power / mass)
P	=	power
PSFC	=	power specific fuel consumption (fuel flow rate per unit power)
r	=	distance or range
R	=	residual (equation to be driven to zero)
S_{ref}	=	wing reference area
SLSQP	=	sequential least squares programming
T	=	thrust force
t	=	time
TMS	=	thermal management system
TOW	=	takeoff weight
V	=	velocity
V_0	=	airspeed at the start of the takeoff roll
V_1	=	takeoff decision speed
V_2	=	takeoff safety speed (minimum OEI climb speed)
V_R	=	takeoff rotation speed
W	=	weight

I. Introduction

In the last decade, aircraft electric propulsion (EP) has become an important research topic. Established industry firms, startups, government agencies, and academia have all conducted conceptual design studies and flown low-power prototypes. For designers and analysts, aircraft EP technology can cause difficulties with existing analysis tools, because many were developed on the assumption that energy would be stored as only fuel. This paper surveys existing tools for analyzing the mission and economic performance of aircraft with electric propulsion, and describes the development of a new open-source conceptual design tool with efficient gradients, component-level parametric cost models, and basic thermal analysis capabilities.

II. The Electric Aircraft Design Problem

Though the field of aircraft EP is still relatively new, insights have emerged about what makes the EP design problem unique.

Design freedom Electric propulsion removes constraints that limited where conventional propulsors could be placed in an aircraft, due in part to the scaling properties of electric motors [1]. This leads to more degrees of freedom in the tradespace and a higher likelihood of finding unconventional configurations with merit.

Close coupling Designers are using electric propulsion for boundary-layer ingestion [2] or lift augmentation [3].

Recent findings indicate that these design features introduce close coupling between aerodynamics and propulsion [4, 5], and between the propulsion, electrical, and thermal management systems [6].

Spatial integration While spatial or geometric integration is important for aircraft design generally, electric propulsion introduces more challenging spatial constraints (such as the volumetric energy density of batteries, which is 18 times lower than fuel [7]). The greater design freedom may enable new ways of alleviating spatial constraints.

Constraints outside the "hard" aerosciences Past modeling and optimization studies of conventional transport aircraft [8] generally began with a conventional architecture (such as "tube-and-wing with podded engines") and made incremental changes based on analysis of the traditional aerosciences disciplines, such as aerodynamics and propulsion. This approach ensures that regulatory, operational, and safety requirements can be satisfied during the detailed design phase without having to model them during conceptual design. With a greatly expanded tradespace and little historical data, each new EP aircraft architecture must be analyzed for safety, operational feasibility, and cost.

Thermal constraints Conventional propulsors generally benefit from exhausting their waste heat into the free stream. Although EP is generally highly efficient, MW-scale electrical power systems generate significant waste heat, which must be managed locally and at the airplane level [6]. Thermal constraints are time- and path-dependent [9]. The weight, cost, and power consumption of the thermal management systems (TMS) necessary to handle this waste heat cannot be adequately addressed using empirical data on conventional environmental control systems. The weight of TMS alone can be significant—as much as 5% of the weight of the entire EP system even at low power levels [10].

These features of the electric propulsion design problem introduce competing requirements for models. Low-cost, moderate-fidelity analysis is necessary in order to explore the broad tradespace; high-fidelity analysis and optimization is necessary in order to explore close coupling and spatial integration.

III. State-of-the-art in Electric Aircraft Analysis

While "textbook" methods and computer codes for conceptual aircraft design have been refined over decades, fundamental assumptions of their formulas and empirical datasets break down when electric propulsion is introduced. For example, the Breguet range equation no longer applies when battery power is used [7]. The problem is particularly pronounced in the area of mission analysis, performance, and sizing codes (admittedly, an imprecise/broad category).

Some researchers have attempted to adapt existing computational tools (based on combustable fuels) to the EP problem. Perullo et al. [11] and Gladin et al. [12] adapted NPSS (an engine cycle modeling environment) by adding medium-fidelity electrical component models. Welstead et al. [13] managed to work around limitations in the time-tested aircraft performance code FLOPS during the trade study for the X-57.

Nevertheless, the trend seems to be to develop built-for-purpose analysis tools to handle the EP problem. At the "textbook" end of the spectrum, Bauhaus Luftfahrt has developed closed-form expressions for electric aircraft sizing [14]. In the realm of analysis codes, NASA has abandoned FLOPS for future EP studies, opting to develop a new code, LEAPS, which natively supports mission analysis using energy from non-fuel sources [13]. At the same time, individual NASA projects have developed their own EP models [9, 15, 16].

Table 1 summarizes the major, published electric fixed-wing aircraft analysis frameworks, color-coded by level of fidelity (there are most probably other frameworks in industry that are not public). The table notably excludes electric VTOL modeling frameworks, which have generally been either low-fidelity or proprietary [17, 18]. Table 1 shows that certain disciplines have received a great deal of attention (electrical, propulsion), while nearly no cost modeling has been incorporated (though one-off studies have tackled the issue [18]). While one-off safety analyses have been conducted, safety has not been incorporated into the analysis process in an automated fashion.

There is significant duplication of effort in the research community, particularly within the area of electrical system modeling and mission analysis. Several codes with similar levels of fidelity for integrating energy used over a mission have been announced [9, 13, 16, 19–25], but none have been open-sourced or made publicly available (with the exception of Stanford's SUAVE, which includes some support for EP modeling). NASA's LEAPS is being developed with the intention of open-sourcing the code, but the release timeline is not clear [13].

A current capability gap is that no publicly-available EP mission analysis and sizing code supports thermal analysis. Multiple industry and government studies have already demonstrated the need to include thermal constraints in analysis and optimization at the conceptual level [6, 9, 19, 26]. Although the LEAPS energy integration method supports electrical and fuel energy storage options, thermal analysis is not included.

Table 1 Electric aircraft modeling and simulation [27]

	GT-HEAT [11, 12, 19]	**NASA X-57**	**NASA N-3X**	**ESAero [28]**	**Bauhaus Luftfahrt**
Aerodynamics	FLOPS/drag polar; BLI benefit based on flat-plate momentum thickness	Design using vortex lattice/boundary layer codes; some CFD for analysis [3, 16, 29]	CFD results from similar configuration, with increment for BLI [30]	Drag polar	L/D correction methods from Torenbeek [31]
Structures	NA	6 DOF beam FEM [16]	NA	NA (for MDAO); detailed analysis of split-wing published in NASA report	NA
Weights	FLOPS tops-down methods	Parametric wing weight (from Raymer) [3], sized beam model [16]	WATE for propulsion flowpaths; tops-down kg/kW estimates for electrics/TMS [15, 32]	WATE for fan weight [33]; low-fidelity radiator model; tops-down empirical for all others	Semi-empirical structural methods; tops-down kg/kW methods for electrics [14]
GNC	Engine, motor, TMS control variables for on- and off-design analysis	Full-mission optimal control [9]	NA; some discussion of off-design conditions in [34]	NA	NA
Electrical	Moderate fidelity motor/inverter loss modeling; equivalent-circuit battery	Transient battery model based on Thevenin equiv circuits (cell-level). Assumed efficiencies for wire/motors [9]	Conceptual: efficiency stackup method with estimates for future tech. Transient: RLC circuit model in SimPowerSystems [15, 35]	Efficiency stackup; battery model unclear	Low-fidelity efficiency stackup with empirical battery discharge curve [14]
Turbo/Propulsion	NPSS	Propeller map from manuf.; prop efficiency from theory [9], blade element momentum theory [16]	NPSS [36]	2D fan analysis using velocity triangles [33]; efficiency maps for turbomachinery	Single prop efficiency parameter [14]
Thermal	TMS sizing considering various heat sources and types of heat sinks	Analytical model for optimization; thermal FEM of motor [9, 37]	Coolant system load based on efficiency stackup (assume 100% to heat) [15]	Cooling based on flight cond. [38]; TMS model discussed in [6]	NA
Operating Cost	NA except for fuel/energy	NA except for fuel/energy	NA	NA	Considers relative cost of fuel/elec; cash operating cost [39]
Noise	NA	NA	ANOPP noise simulation prompted redesign [32]	NA	NA
Safety	NA	Comprehensive FMEA [40, 41]	FMEA and FTA for loss of thrust; more work needed for other hazards [42, 43]	Qualitative	NA

The open-source SUAVE conceptual design tool also does not incorporate thermal management analyses.

Another need exists for an EP model with efficient gradients. When high-fidelity disciplinary analysis codes and hundreds of design variables are used, the computational cost can be minimized by using gradient-based optimization [44]. However, using finite-difference gradients significantly increases computational cost. SUAVE does not support analytic or automatic gradients, and it does not appear that LEAPS will either. Other NASA electric aircraft studies demonstrate the benefits of efficient gradients in mission analysis codes [9, 16].

Falck et al. [9], and Hwang and Ning [16] developed electric aircraft mission analysis codes with moderate fidelity and efficient gradients. The two codes are similar and rely on optimal control theory and collocation methods to calculate trajectories, energy usage, and thermal states. Using OpenMDAO, the codes provide efficient gradients for use in large scale optimization [16]. However, optimal control-based methods sometimes introduce robustness problems. For example, the problem may not converge if initial guesses of the states and trajectories are not close enough. There may also be cases where non-optimal trajectories form constraints on the design problem (e.g., whenever a human pilot is in the loop). Neither model supports parametric cost estimates, and neither model is currently publicly available.

Therefore, a need exists for an electric aircraft mission performance and sizing tool with:

- Thermal analysis
- Component-based parametric cost
- Public availability
- Efficient gradients for use with high-fidelity multidisciplinary design optimization (MDO)

To meet these needs, we introduce our conceptual design toolkit, under the working title "OpenConcept". OpenConcept is a Python-based library built on top of the NASA-led OpenMDAO 2 framework [45, 46]. At the highest level, it consists of three parts: a library of propulsion modeling components; a set of reusable, analytically-differentiated mission analysis codes; and a set of example aircraft models capable of analysis only, simple resizing, or full MDO.

IV. Propulsion Models

We have developed a set of simple conceptual-level electrical and turbomachinery models based on OpenMDAO's `ExplicitComponent` class. These can be connected together to form all-electric, conventional, series hybrid, parallel hybrid, or turboelectric architectures. We currently have developed:

- `SimpleBattery`: electrical power source with constant specific power and specific energy
- `SimpleMotor`:constant assumed efficiency
- `SimpleGenerator`: constant assumed efficiency
- `SimpleTurboshaft`: constant assumed power-specific fuel consumption (PSFC)
- `SimplePropeller`: shaft power to thrust based on empirical efficiency map
- `Splitter`: combines or divides power sources or loads

Each component has one or more required scalar sizing design variables (such as motor horsepower or battery weight), which remain constant throughout the mission. The components also use vectorized inputs and outputs, such as throttle setting or shaft power in. The user may optionally override default technology parameters (representative of the state-of-the-art today) with different assumptions (e.g., cost per motor kW, or battery specific energy).

Vectorization is an important concept in OpenMDAO. Instead of invoking a model function once for each flight condition with scalar inputs, all of the flight conditions for all of the analysis points are fed in at once as `numpy` vectors, and model computations are handled as vectorized operations. This is a good design practice in Python, since repetitive computation is performed by the compiled `numpy` code. While we made the design decision not to use an optimal control formalism for our mission analysis code, our vectorized propulsion model components are fully compatible with NASA Glenn's soon-to-be open source optimal control tool, Dymos, which also runs on top of OpenMDAO.

Our design philosophy is that, in general, mechanical components "push" and electrical components "pull". A turboshaft engine pushes shaft power proportional to its rated power and throttle setting. An electrical motor pushes shaft power in the same way, but also pulls an electrical power demand on any connected upstream source, which might include a generator or a battery.

Where mechanical power (typically, a turboshaft) drives a generator, there is an implicit gap where power in must equal power out. OpenConcept uses a Newton solver to find the throttle setting for the engine by driving the following residual equation to zero at every flight condition:

$$\vec{R}_{\text{gen}} = \vec{P}_{\text{gen}} - \vec{P}_{\text{req}} \tag{1}$$

Figure 1 shows a twin-motor series hybrid propulsion system built in OpenConcept and used for the case study in

Section VI. The "examples" folder of the first software release will contain the code for this architecture as well as single and twin engine conventional turboprop architectures.

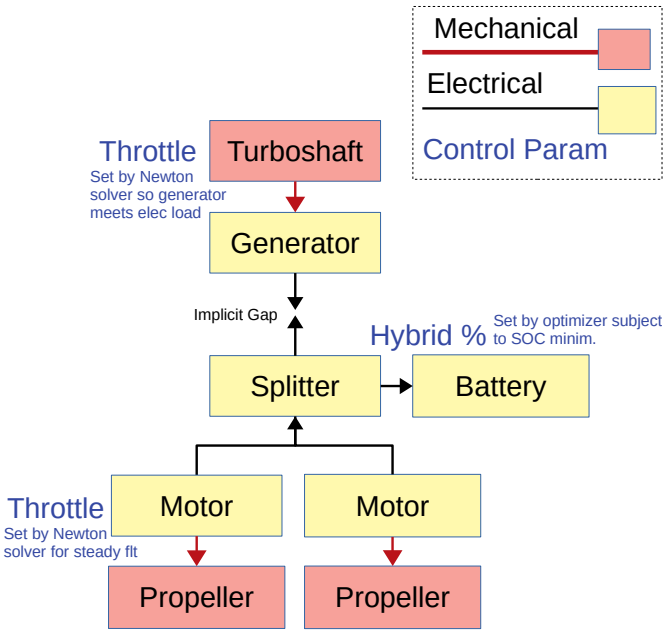

Fig. 1 Example of a twin-motor series hybrid electric propulsion model in OpenConcept.

Each component also provides outputs useful for economic optimization or thermal analysis:

- `heat_out` (vector) tracks the waste heat produced by the component at each flight condition based on the current operating power and the component efficiency.
- `component_sizing_margin` (vector) is P/P_{rated} at each flight condition.
- `component_cost` (scalar) represents the non-recurring cost of the component in USD.
- `component_weight` (scalar) is the component's contribution to airplane empty weight

The `Simple` components generate heat at a rate proportional to their instantaneous power level and their (constant) inefficiency. They also have linear cost and weight estimates based on the rated power and technological assumptions. Structuring weight, cost, and thermal data in a standard way makes it simple to connect analysis tools to entire propulsion layouts.

While OpenConcept is not multifidelity, it is simple for a user to increase model fidelity in a modular way as an aircraft's design matures. Using OpenMDAO's native surrogate modeling classes, it is easy to upgrade the simple constant performance models with empirical data and maintain accurate partial derivatives. We validated this with the `SimplePropeller` component, which uses empirical propulsive efficiency data at a grid of advance ratios and power coefficients (Figure 4). For example, future users may easily upgrade the motor component with a proprietary efficiency map based on RPM and torque. However, care must be taken to only use empirical data when the domain of data is large. Newton solvers and optimizers have a tendency to walk outside the bounds of a surrogate model which can cause convergence failures.

The `Simple` components can also be replaced with more complex physics-based OpenMDAO models, as long as they have accurate and efficient partial derivatives. For example, pyCycle is an OpenMDAO-based cycle analysis tool similar to NPSS. pyCycle can, in principle, accept flight conditions and control inputs from OpenConcept and return medium-fidelity fuel flows and thrusts [47, 48]. Blade element momentum theory propeller modeling was implemented in OpenMDAO in [16]. Compiled non-OpenMDAO codes can be "wrapped" in OpenMDAO.

Upcoming work will greatly extend the thermal analysis and design capabilities of OpenConcept, including tracking component temperatures across mission time points and calculating power required to maintain heat equilibrium using a

cooling system.

V. Analysis Routines

OpenConcept currently has two primary analysis modules: `takeoff` and `mission`. Together, they provide sufficient objective and constraint data to perform conceptual-level sizing and MDO of a wide variety of conventional and unconventional aircraft.

A. Takeoff Analysis

The `takeoff` module calculates balanced field length (BFL) and propulsion system states during the takeoff run, using methods and assumptions presented in [49]. For this flight phase, control inputs are specified by the user (e.g. 100% throttle) and accelerations are determined using a force balance equation. In order to compute balanced field length, `takeoff` divides the takeoff into five segments:

1) Takeoff roll at full power from V_0 to V_1
2) Takeoff roll at one-engine-inoperative (OEI) power from V_1 to V_R
3) Rejected takeoff with zero power and max braking from V_1 to V_0
4) Transition in a steady circular arc to the OEI climb-out flight path angle and speed
5) Steady climb at V_2 speed and OEI power until an obstacle height h_o is reached

During the takeoff roll (segments 1, 2, and 3), the force balance equation is:

$$\frac{d\vec{V}}{dt} = \vec{T} - \vec{D} - \mu(mg - \vec{L}). \tag{2}$$

The accelerate-go distance combines segments 1, 2, 4, and 5, while the accelerate-stop distance includes 1 and 3.

By default, $V_R = 1.1V_{\text{stall}}$ and $V_2 = 1.2V_{\text{stall}}$, where stall speed is calculated by a separate model component as a function of MTOW; these default multipliers (from [49]) can be overridden. V_0 is assumed to be 1 m/s in order to avoid singularities in analysis codes at zero forward speed. Default μ is 0.03 during the takeoff roll, and 0.4 during emergency braking in a rejected takeoff, though this can be also be overridden to simulate wet or snowy runways or improved aircraft brake systems. The obstacle clearance height is set at 35 feet by default (14 CFR 23), but can be trivially changed to 50 feet to model a Part 25 transport aircraft.

Equation (2) is an ordinary differential equation and must be integrated to obtain distances for segments 1, 2 and 3. For example, the distance travelled during run up to decision speed (segment 1) is:

$$R_{V_1} = \int_{V_0}^{V_1} \frac{dr}{dt}\frac{dt}{dV}\, dV = \int_{V_0}^{V_1} \frac{V}{a}\, dV. \tag{3}$$

OpenConcept uses an implementation of Simpson's Rule for numerical integration with analytic derivatives. An integral can be approximated using Simpson's rule as follows:

$$\int_{x_L}^{x_U} f(x)\, dx \approx \frac{1}{3}\Delta x(f_0 + 4f_1 + 2f_2 + 4f_3 + 2f_5 + \ldots + 2f_{2N-2} + 4f_{2N-1} + f_{2N}) \tag{4}$$

$$\Delta x = \frac{x_U - x_L}{2N}, \tag{5}$$

where N is the number of Simpson subintervals and Δx is the constant spacing between the points $\vec{f}$. This method always requires evaluating a function at $2N + 1$ points. Simpson's rule integrates polynomials up to third order exactly [50].

Integration requires known endpoints of the differential variable. During the takeoff phase, OpenConcept 'knows' the indicated airspeeds (V_0,V_1,V_R) and integrates numerically with respect to dV over each segment. Since acceleration depends on drag, which depends on velocity but is not time dependent, the acceleration can be computed over a equally-spaced range of velocities and then integrated using Simpson's rule.

The `takeoff` module uses a Newton solver to vary the chosen V_1 speed until the accelerate-go and accelerate-stop distances are equal, or until the accelerate-go distance is longer than the accelerate-stop distance and $V_1 = V_R$. The accelerate-go distance is then equal to the *balanced field length*, which can be used as an optimization or sizing constraint.

The takeoff module does not consider the slight change in aircraft weight as fuel is burned during takeoff, but it does track the total fuel (and electricity, if applicable) consumed during the takeoff roll. A limitation of integration with respect to velocity is that spuriously low takeoff field length results may occur when negative accelerations are fed to the integrator. This only occurs when the aircraft cannot physically accelerate through the limits of integration. OpenConcept provides a helper function, `takeoff_check`, to verify that all accelerations are positive during the takeoff roll. If `takeoff_check` returns an error, the user should specify a higher thrust setting or reduce aircraft weight and drag until takeoff is physically possible.

B. Mission Analysis

The `mission` module accomplishes two main tasks: setting condition-dependent control inputs necessary for steady flight, and integrating quantities such as fuel burn and energy over the mission profile. An OpenConcept mission currently consists of three segments, but can easily be extended to six to include a reserve mission:

- Climb at constant vertical speed and indicated airspeed to the cruise altitude.
- Cruise at constant indicated airspeed and altitude.
- Descent at constant indicated airspeed and vertical speed to the landing altitude.

Figure 2 illustrates flight conditions and aircraft states for a representative hybrid-electric aircraft mission.

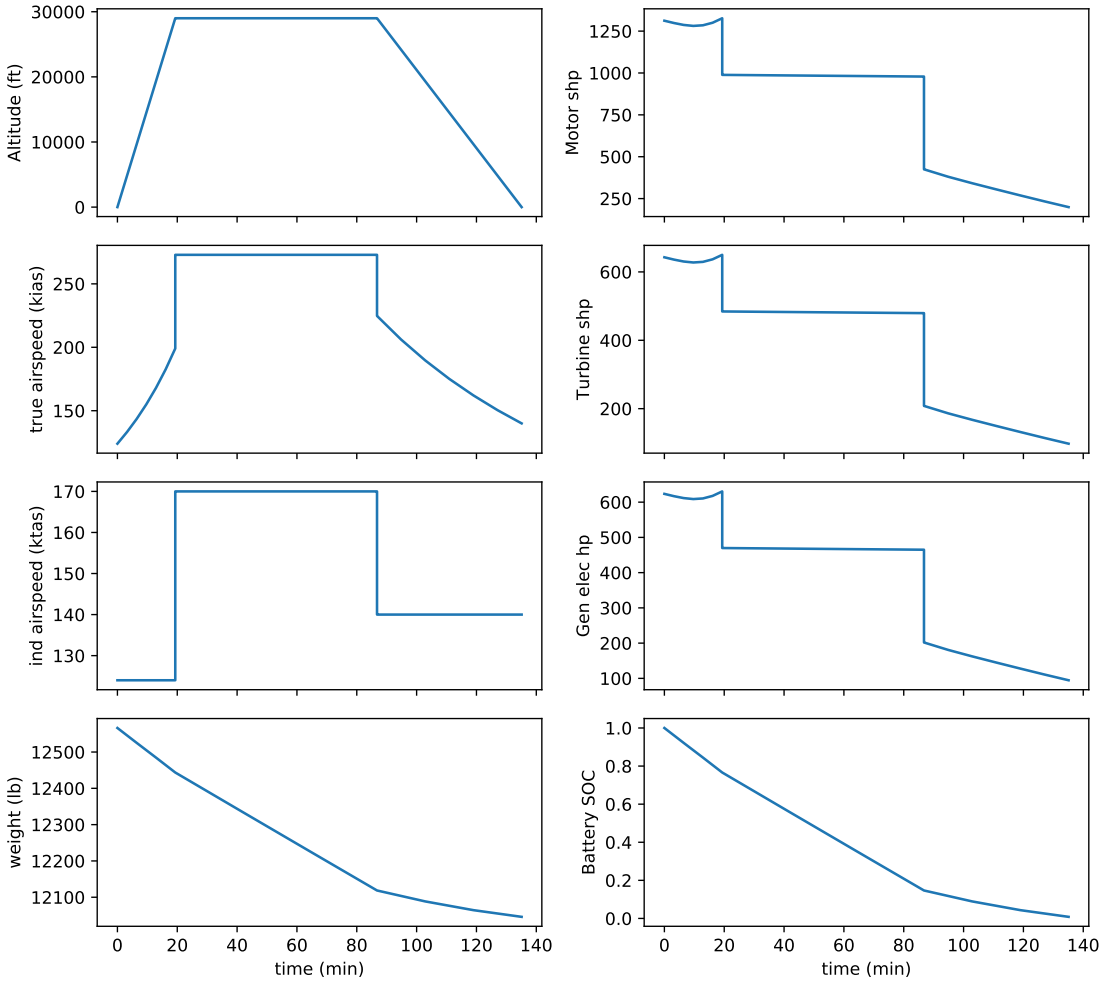

Fig. 2 Representative mission profile (from Section VI case study; e_b = 500 Wh/kg, range= 500 nmi)

During mission analysis, the aircraft is treated as a point mass, which changes as fuel burns. At each flight condition,

the `mission.ThrustResidual` component calculates the value of the residual equation

$$\vec{R}_{\text{thrust}} = \vec{T} - \vec{D} - \vec{m}g\sin(\vec{\gamma}). \tag{6}$$

OpenMDAO's Newton solver drives these residuals to zero at every flight condition in the mission by varying the primary thrust control parameter (usually either motor or engine throttle). If more than one independent thrust control parameter is available (for example, high-lift and cruise propellers as in the X-57), the user can specify some of the parameters and let the Newton solver find the remaining one. Alternatively, an optimizer can find the optimal value for every control parameter by treating the thrust residual as an equality constraint.

The steps in an OpenConcept mission analysis during each Newton iteration are:

1) Generate vectors representing the flight condition at each point in time during the mission.
2) Calculate atmospheric properties [51].
3) Compute climb and descent phase distances and times to obtain cruise distance and time.
4) Run an OpenConcept propulsion model at each flight condition to obtain fuel flows, battery loads, thrusts, and constrained quantities like heat output.
5) Integrate fuel flow and battery load with respect to time using Simpson's rule to obtain aircraft weight and battery state of charge (SOC) vectors.
6) Calculate flight C_L and drag.
7) Calculate the thrust-drag residual.

Many conventional mission analysis codes include mission range as an output, assuming that the aircraft will fly until the fuel weight is zero. OpenConcept uses mission range as an *input*, since the limiting all-electric case has no change in weight to integrate. Therefore, the cruise phase range and time depend on the climb and descent phases as well as the specified total range. Because of the current mission specification scheme, OpenConcept "knows" the beginning and end time points of each phase; fuel and battery states are then integrated with respect to time using Simpson's rule. An alternative, more flexible integration strategy could include integrating with respect to altitude for the climb and descent segments, and with respect to distance for the cruise segment.

Once the Newton solver has converged the mission, thrust balances drag (and weight, if climbing or descending), lift matches weight, and any hybrid turbomachinery components are producing the correct shaft power to meet electrical loads.

The `mission.ComputeMissionResiduals` component then assesses whether the aircraft's design weights are consistent with the mission being flown. The residuals are:

$$\begin{aligned} R_{\text{TOW}} &= W_{\text{TO}} - W_{\text{fuel}} - W_{\text{empty}} - W_{\text{payload}} \\ R_{\text{vol}} &= W_{\text{fuel,max}} - W_{\text{fuel}}. \end{aligned} \tag{7}$$

For aircraft with batteries, the `mission.ComputeMissionResidualsBattery` class should be used instead. In this case, the residuals are:

$$\begin{aligned} R_{\text{TOW}} &= W_{\text{TO}} - W_{\text{fuel}} - W_{\text{empty}} - W_{\text{payload}} - W_{\text{batt}} \\ R_{\text{batt}} &= E_{\text{batt,max}} - E_{\text{batt,used}} \\ R_{\text{vol}} &= W_{\text{fuel,max}} - W_{\text{fuel}} \end{aligned} \tag{8}$$

The Newton solver does not automatically drive these high-level equations to zero, which enables analysis of aircraft where not all of the fuel or battery is consumed during a mission. However, it can be convenient to use OpenConcept in "sizing" mode, where these residuals are posed as inequality constraints to the optimizer. TOW and battery weight are then set to the minimum required to fly the mission. When using the `mission` module without an optimizer in the loop, the user must manually ensure that the mission weights are feasible.

Partial derivatives for all of the `mission` analysis methods have been verified using OpenMDAO's `check_partials` method. Users of OpenConcept should *always* verify partial derivatives when implementing new components or modifying existing ones. Simple errors in partial derivatives inevitably cause major Newton and optimizer convergence issues.

The number of Simpson subintevals in each mission segment is a major driver of the size of the linear algebra problem solved by OpenMDAO. We performed a convergence study of the integration method using a representative hybrid aircraft model which uses significant battery and fuel energy (described in Section VI). Table 2 illustrates that very accurate fuel burn and BFL results can be obtained with a relatively minimal number of points per mission segment. Five intervals per segment is the default and integrates fuel burn and BFL nearly exactly; using three intervals runs significantly faster and may be a good lower bound for running numerous optimizations.

Table 2 Simpson integration convergence

Simpson Intervals	Points	Fuel Burn	FB Error	BFL	BFL Error
15	31	**314.18975**	0.000%	**1357.0047**	0.00%
8	17	**314.18975**	0.000%	**1357.0047**	0.00%
5	11	**314.19**058	0.000%	**1357.00**53	0.00%
4	9	**314.19**259	0.001%	**1357**.1920	0.01%
3	7	**314.19**254	0.001%	**1357**.2149	0.02%
2	5	**314.19**330	0.001%	**135**6.2602	−0.05%
1	3	**314**.31917	0.041%	**1357**.5849	0.04%

VI. Case Study: Design of an Electric Aircraft for Minimum Operating Cost

To validate the code, we conducted a case study where the notional goal is to convert a Beechcraft King Air C90GT to series hybrid electric propulsion.

A. Conventional Baseline

To test OpenConcept's propulsion modeling and analysis routines on a simple case, we first modeled a single engine turboprop, the SOCATA/Daher TBM 850. Structural and system weights were estimated using textbook formulas [49, 52], with a constant factor of 1.6 applied to structural weight in order to match published empty weights [53]. Cruise drag was estimated using a drag polar formulation, with induced drag and zero-lift drag estimated using tops-down methods [49]. $C_{L\max}$ was set to match the nominal takeoff rotation speed to handbook values [54]. Initial model runs using the *a priori* estimate of C_{D_0} resulted in a fuel burn total close to the published value; we adjusted C_{D_0} to match fuel burn and maximum range.

Propeller maps from manufacturers are closely held. For our case study, propeller efficiency was estimated from a published map [55]. We "compressed" this map in the C_P axis so that the peak efficiency point better matched our anticipated operating point, and visually extrapolated the map into the higher C_P region. We also adjusted the very low speed propulsive efficiency downward to reduce spuriously high thrust levels during the takeoff roll. The balanced field length for the single-engine TBM is simply the takeoff distance with full takeoff power since the one-engine-inoperative takeoff distance is not defined.

We modeled the Beechcraft King Air C90GT in a nearly identical way, except that the King Air has two engine and propeller components and a structural factor of 2.0 [56]. On the King Air, the PT6A-135A engine is derated by about 25% (from 750 hp to 550 hp) for structural reasons. Balanced field length was calculated using 25% derated takeoff power, and zero power in Engine 2 following V_1. Table 4 illustrates input and model output data for the TBM 850 and King Air. Balanced field length for the King Air matched published figures quite closely, but the simulated fuel burn was about 25% lower. It is possible that the propeller map is not representative of the King Air at the cruise flight condition, or that in reality the derated PT6A-135A engine is operating significantly below peak efficiency at our cruise throttle setting and altitude. We did not attempt to vary C_{D0} upward enough to match the published (higher) fuel burn for the King Air.

(a) Daher TBM 850 (photo by Gyrostat, CC-BY-SA)

(b) Beechcraft King Air C90GTi (photo by Joao Carlos Medau, CC-BY)

Fig. 3 OpenConcept benchmark aircraft

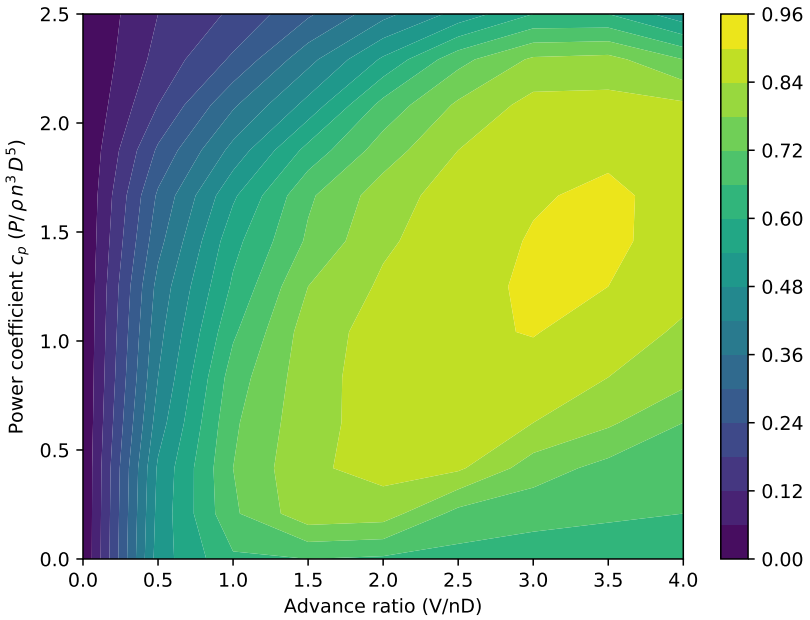

Fig. 4 Propeller efficiency map for the case study (notional; not to be used for industry studies).

B. Sizing the Propulsion System of a Series-Hybrid Conversion

Next, we examine the feasibility of a drop-in replacement of the twin turboprop architecture of the King Air with a series hybrid system. The pupose of this study is *not* to prove or disprove the viability of electric propulsion for light aircraft retrofit; we are simply illustrating the use of OpenConcept for an aircraft study. A modern clean-sheet design would have weight and drag advantages which may make electric propulsion feasible at longer ranges and lower e_b.

We assume that any single component of the propulsion system may fail and that the aircraft must be able to continue safe flight and landing during the takeoff phase. To achieve this, the series hybrid architecture includes the following features:

- Two motors and propellers (providing redundancy in the event of motor or propeller failure)
- Batteries split into at least two independent packs, with battery power alone used for takeoff (providing redundancy against single engine failure on takeoff)

These conditions ensure a level of safety on takeoff equivalent to a twin turboprop. Specific power, efficiency, and cost

assumptions for individual powertrain components are stated in Table 3.

Table 3 Powertrain technology assumptions

Component	Specific Power (kW/kg)	Efficiency	Cost	PSFC (lb/hp/hr)
Battery	5.0	–	\$50/kg	–
Motor	5.0	97%	\$100/hp	–
Generator	5.0	97%	\$100/hp	–
Turboshaft/Prop	7.15*	–	\$775/shp	0.6

The `scipy.optimize` SLSQP algorithm was used to size the propulsion system components (motor, engine, and generator sizing) for minimum fuel burn on the design mission. MTOW, wing area, and all other parameters remain equal to the King Air baseline. The optimization problem is formulated as:

$$
\begin{aligned}
\text{minimize: } & \text{fuel burn} \\
\text{by varying: } & \\
& W_{\text{battery}} \\
& P_{\text{motor}} \text{ (rated)} \\
& P_{\text{turboshaft}} \text{ (rated)} \\
& P_{\text{generator}} \text{ (rated)} \\
& H_E \text{ (degree of hybridization w.r.t energy)} \\
\text{subject to scalar constraints: } & \\
& R_{\text{TOW}} = W_{\text{TO}} - W_{\text{fuel}} - W_{\text{empty}} - W_{\text{payload}} - W_{\text{batt}} \geq 0 \\
& R_{\text{batt}} = E_{\text{batt,max}} - E_{\text{batt,used}} \geq 0 \\
& \text{BFL} \leq 4452 \text{ ft (no worse than baseline)} \\
\text{and vector constraints: } & \\
& \vec{P}_{\text{motor}} \leq 1.05 P_{\text{motor}} \text{ (rated)} \\
& \vec{P}_{\text{turboshaft}} \leq P_{\text{turboshaft}} \text{ (rated)} \\
& \vec{P}_{\text{generator}} \leq P_{\text{generator}} \text{ (rated)} \\
& \vec{P}_{\text{battery}} \leq W_{\text{battery}} \cdot p_b
\end{aligned}
$$

The optimizer successfully sized the motor, generator, battery, and turboshaft and found the mix of electric and fuel energy (*degree of hybridization*, H_E) which minimized fuel burn. Design variables and simulation outputs are listed in Table 4. Using battery specific energy of 750 Wh/kg, the series conversion could not meet the 1000nmi design range of the original King Air. At a maximum range of 762 nmi, the optimizer converged on a design with essentially the minimum allowable amount of battery (sized by power, not energy, at takeoff). Since the 762 nmi mission was at the very limit of the airplane's capability, we changed the design range to 500 nmi and resized the propulsion system again. This time, e_b significantly affected the sizing (at 250, 500, and 750 Wh/kg). All three designs had identical motor sizing (to meet the takeoff constraint at MTOW), but the generators and engine power increased with decreasing e_b due to the larger fraction of power from fuel. The 750 Wh/kg case burned 38% less fuel than the 250 Wh/kg case.

To further validate the speed and flexibility of OpenConcept, the first author conducted a rough feasibility study of an all-electric conversion of the Cessna C208B Grand Caravan. The objective was to assess the feasibility of using all-electric propulsion to handle cargo flights of one hour or less, as proposed by the start-up firm MagniX. From start to finish (including gathering input data on the Grand Caravan online and assessing control surface areas using photogrammetric methods), the study took less than 90 minutes. The results are not tabulated here, but indicated that the idea could be feasible with current technology.

*does not include 104kg base wt

C. Multidisciplinary Design Optimization for Minimum Fuel Burn

Following successful demonstration of the simple sizing capability, we increased the design freedom of the optimizer to include MTOW, fuel volume, wing area, and prop diameter. The optimization problem is:

$$\begin{aligned}
\text{minimize: } & \text{fuel burn} + 0.01 MTOW \\
\text{by varying: } & \\
& \text{MTOW} \\
& S_{ref} \\
& d_{prop} \\
& W_{\text{battery}} \\
& P_{\text{motor}} \text{ (rated)} \\
& P_{\text{turboshaft}} \text{ (rated)} \\
& P_{\text{generator}} \text{ (rated)} \\
& H_E \text{ (degree of hybridization w.r.t energy)} \\
\text{subject to scalar constraints: } & \\
& R_{\text{TOW}} = W_{\text{TO}} - W_{\text{fuel}} - W_{\text{empty}} - W_{\text{payload}} - W_{\text{batt}} \geq 0 \\
& R_{\text{batt}} = E_{\text{batt,max}} - E_{\text{batt,used}} \geq 0 \\
& R_{\text{vol}} = W_{\text{fuel,max}} - W_{\text{fuel}} \geq 0 \\
& \text{BFL} \leq 4452 \text{ ft (no worse than baseline)} \\
& V_{\text{stall}} \leq 81.6 \text{ kt (no worse than baseline)} \\
\text{and vector constraints: } & \\
& \vec{P}_{\text{motor}} \leq 1.05 P_{\text{motor}} \text{ (rated)} \\
& \vec{P}_{\text{turboshaft}} \leq P_{\text{turboshaft}} \text{ (rated)} \\
& \vec{P}_{\text{generator}} \leq P_{\text{generator}} \text{ (rated)} \\
& \vec{P}_{\text{battery}} \leq W_{\text{battery}} \cdot p_b
\end{aligned}$$

Results for 250, 500, 750, and 1000 Wh/kg on a 500 nmi design mission are listed in Table 4. In these four optimizations, we see some hints of discontinuities in the hybrid electric design space. At 1000 and 750 Wh/kg, the airplane prefers to use no fuel and fly the design mission completely on batteries. At 500 Wh/kg, the optimizer hits the MTOW upper bound (5700kg, above which EASA and the FAA require pilots to obtain a type rating). It uses as much battery as possible, supplementing with just enough fuel to meet the required range. At 250 Wh/kg, the optimizer prefers to reduce battery weight to the takeoff power-constrained minimum and *reduce* MTOW below the baseline.

This fuel burn optimization was repeated over a grid of 252 individual combinations of design range and e_b (Figure 5). Only one out of 252 optimization runs failed to converge, and that run was easily rectified by changing the starting "guess" to a more realistic set of design weights and component sizes.

The primary finding from this set of optimizations is that, for an airplane with King Air-like structural efficiency and aerodynamics, hybrid propulsion is generally only preferable to all-fuel or all-electric operation when an upper limit exists on MTOW. Practical MTOW limits might include a retrofit application with an existing airframe, or regulatory limits (as mentioned above). This finding may not apply generally to more aerodynamically and structurally efficient clean-sheet designs.

In the upper left corner (short range, high e_b), the optimizer can eliminate fuel altogether. Since fuel burn is zero everywhere in this triangular region, using pure fuel burn as the objective function will fail to converge on a reasonable airplane. A small additional term proportional to MTOW was added to the objective function in order to encourage the optimizer to reduce MTOW (and therefore, battery weight) as much as possible, once fuel burn is reduced to zero.

D. Multidisciplinary Design Optimization for Minimum Cost

We ran an additional grid of 252 optimizations with respect to operating cost. The optimization problem is formulated as follows:

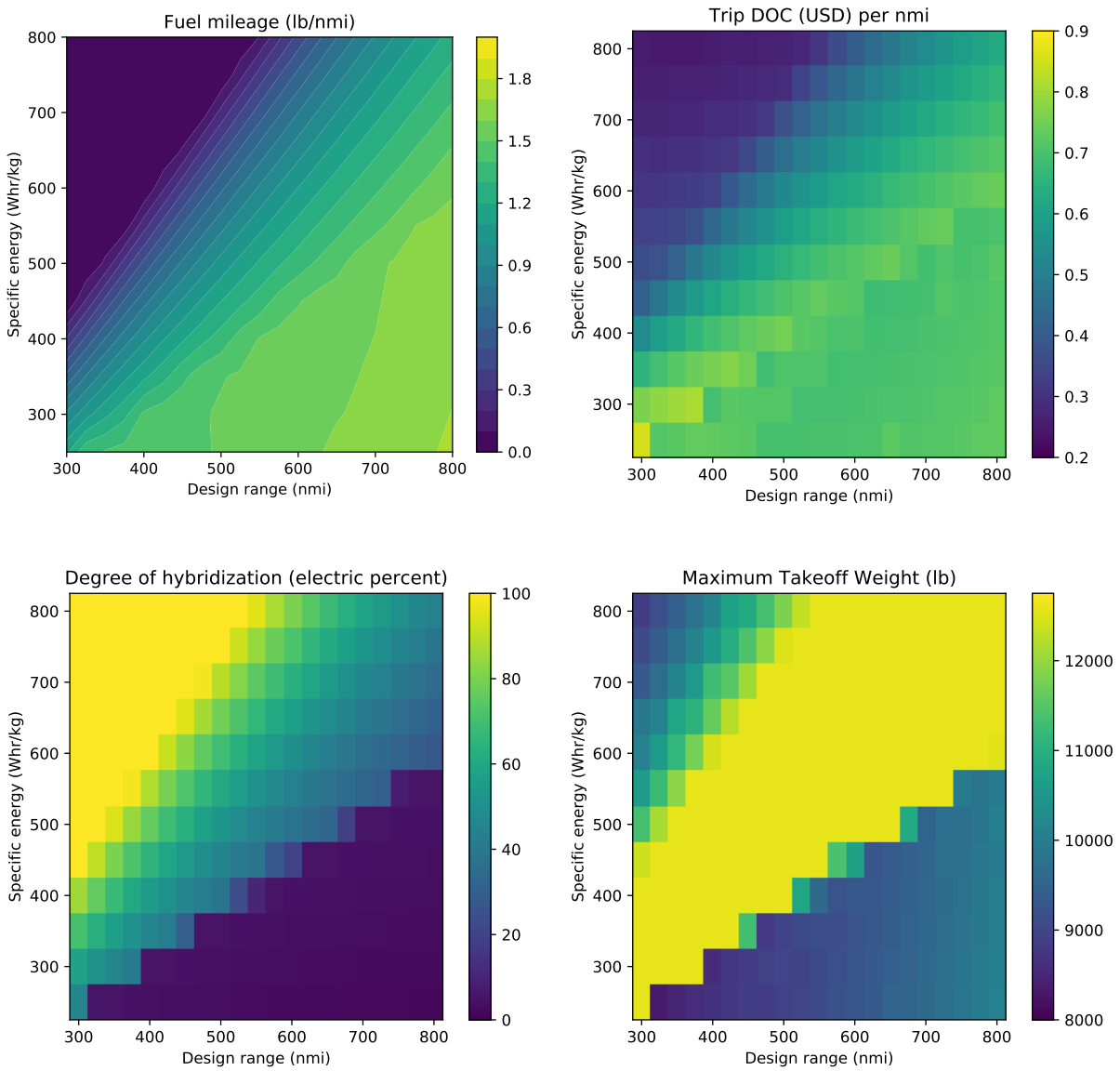

Fig. 5 Minimum fuel burn MDO results.

$$
\begin{aligned}
\text{minimize: } & \text{trip cost} \\
\text{by varying: } & \\
& \text{MTOW} \\
& S_{ref} \\
& d_{prop} \\
& W_{\text{battery}} \\
& P_{\text{motor}} \text{ (rated)} \\
& P_{\text{turboshaft}} \text{ (rated)} \\
& P_{\text{generator}} \text{ (rated)} \\
& H_E \text{ (degree of hybridization w.r.t energy)}
\end{aligned}
$$

subject to scalar constraints:

$$
\begin{aligned}
R_{\text{TOW}} &= W_{\text{TO}} - W_{\text{fuel}} - W_{\text{empty}} - W_{\text{payload}} - W_{\text{batt}} \geq 0 \\
R_{\text{batt}} &= E_{\text{batt,max}} - E_{\text{batt,used}} \geq 0 \\
R_{\text{vol}} &= W_{\text{fuel,max}} - W_{\text{fuel}} \geq 0 \\
\text{BFL} &\leq 4452 \text{ ft (no worse than baseline)} \\
V_{\text{stall}} &\leq 81.6 \text{ kt (no worse than baseline)}
\end{aligned}
$$

and vector constraints:

$$
\begin{aligned}
\vec{P}_{\text{motor}} &\leq 1.05 P_{\text{motor}} \text{ (rated)} \\
\vec{P}_{\text{turboshaft}} &\leq P_{\text{turboshaft}} \text{ (rated)} \\
\vec{P}_{\text{generator}} &\leq P_{\text{generator}} \text{ (rated)} \\
\vec{P}_{\text{battery}} &\leq W_{\text{battery}} \cdot p_b
\end{aligned}
$$

A notional trip cost model was constructed as follows:

$$
\begin{aligned}
\text{Trip cost} &= c_{\text{fuel}} + c_{\text{electricity}} + c_{\text{battery}} + c_{\text{depreciation}} \\
&\text{where:} \\
c_{\text{fuel}} &= (\$2.50/\text{gal})\, W_{\text{fuel}}/\rho_{\text{fuel}} \\
c_{\text{electricity}} &= (\$36.00/\text{MWh})\, E_{\text{batt, used}} \\
c_{\text{battery}} &= (\$50.00/\text{kg})\, W_{\text{batt}}\, /n_{\text{batt cycles}} \\
c_{\text{depreciation}} &= c_{\text{aircraft}}/n_{\text{flights,daily}}/365 \text{ days}/n_{\text{years}} \\
&\text{and:} \\
c_{\text{aircraft}} &= (\text{OEM premium})\, \left(c_{\text{airframe}} + c_{\text{engine}} + c_{\text{motors}} + c_{\text{generator}}\right) \\
c_{\text{airframe}} &= (\$277/kg)\, \left(\text{OEW} - W_{\text{engines}}\right) \\
c_{\text{engine}} &= (\$775/\text{shp})\, P_{\text{engine}} \text{ (rated)} \\
c_{\text{motors}} &= (\$100/\text{shp})\, P_{\text{motors}} \text{ (rated)} \\
c_{\text{generator}} &= (\$100/\text{shp})\, P_{\text{generator}} \text{ (rated)} \\
n_{\text{batt cycles}} &= 1500 \\
n_{\text{flights,daily}} &= 5 \\
n_{\text{years}} &= 15 \\
\text{OEM premium} &= 1.1
\end{aligned}
$$

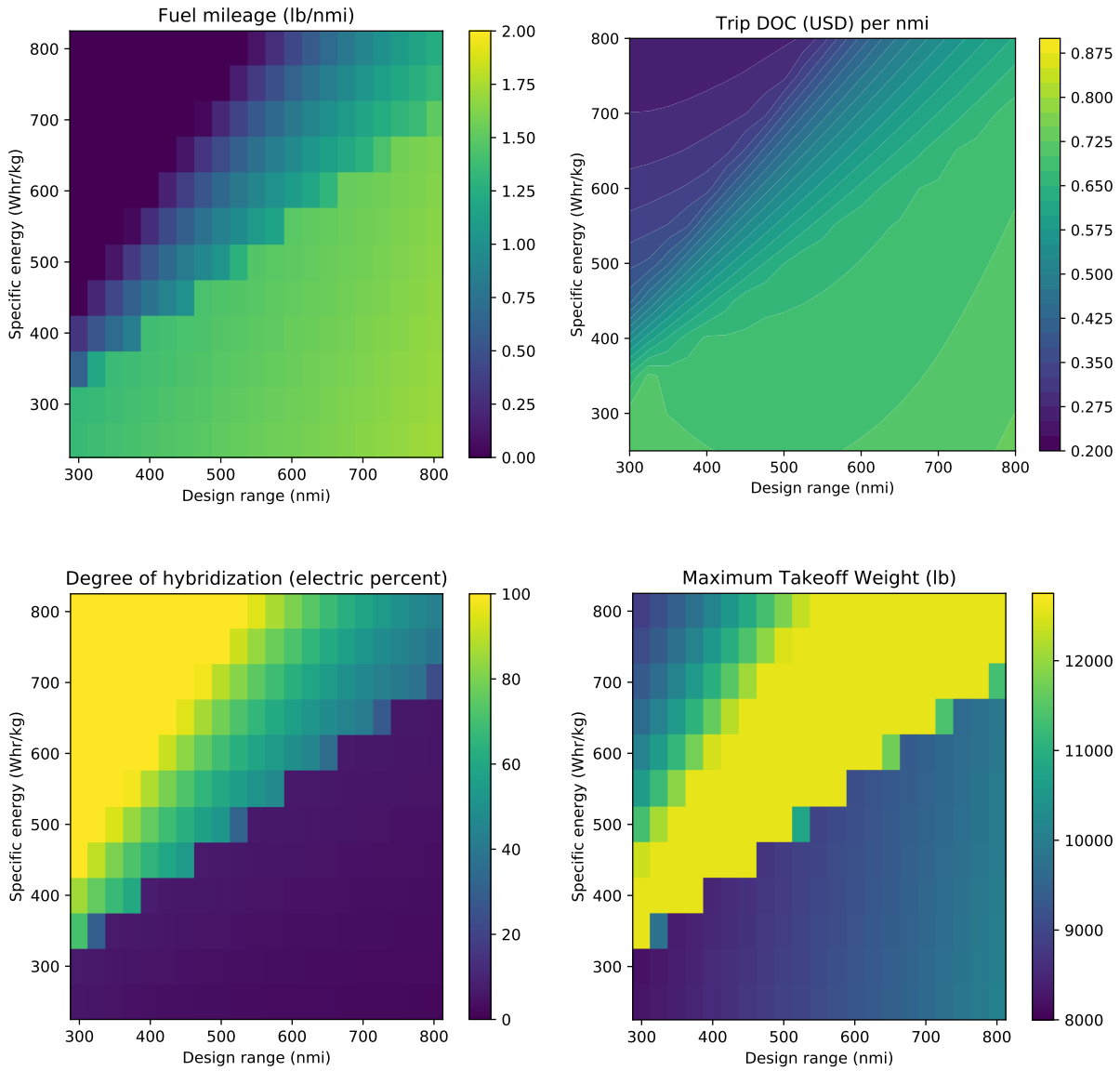

Fig. 6 Minimum Cost MDO Results

Fuel and electricity prices were picked as representative wholesale values for 2018. Battery cost was estimated assuming $200 per kWh, and specific energy of 250 Wh/kg. Airframe cost factor includes everything except propulsion components and was estimated based on general light turboprop pricing trends (in current USD currency) Engine price per shaft horsepower was estimated based on new PT6A prices listed on various online marketplaces. The OEM premium assumes a 10% operating profit above Tier 1 supplier costs. Note that the cost model does *not* contain any contribution from maintenance cost (for either conventional or electric propulsion), nor does it include crew costs or landing fees. Crew cost is neglected, as the missions being tested are equal in block time. Maintenance and crew cost could be easily added to the cost calculation for future studies.

The price of aerospace-certified propulsion motors and generators, and the cycle life of aerospace-grade batteries, are all currently unknown since they are not commercially available. The maintenance cost of electric propulsion is also unknown, although it can be expected to be lower than for turboprop engines on an hourly basis. The effect of these economic assumptions on optimal design can be easily tested using OpenConcept.

Figure 6 shows the cost, fuel burn, degree of hybridization, and MTOW for the cost-optimized aircraft. Compared to Figure 5, optimizing for cost has moved the electric propulsion feasibility line up and to the left. Under this (debatable) set of economic assumptions, electric propulsion is more favorable for fuel burn reduction than for economics, at least at moderate specific energy levels.

We ran an additional 21 optimizations of a King Air-like conventional twin turboprop, but allowed the optimizer to perform full MDO (same rules as for the hybrid MDO study, but without the electric propulsion design varibles or constraints). The purpose of these cases was to provide a fair comparison between a conventional architecture and the series hybrid architecture. Figure 7 shows the relative difference between the cost-optimzed hybrid electric aircraft compared to cost-optimized coventional aircraft at the same design range. In the lower right half, the series hybrid (effectively turboelectric) design actually costs more to operate than a conventional twin turboprop. A breakeven point runs nearly linearly from lower left to upper right; conventional and electric are economically equivalent along this line. Above the breakeven line (in the hybrid regime), costs fall rapidly as the optimizer can trade fuel for batteries and reduce the size of the turbogenerator system. Once turbogenerator power is reduced to zero, the (low) costs remain relatively stable even as battery specific energy improves. Figure 7 illustrates that the potential for cost savings is high if a significant proportion of battery power can be used. Turboelectric propulsion by itself is not an efficient replacement for turboprop engines, at least when no ancillary aerodynamic or propulsive efficiency benefit can be realized. If maintenance costs were modeled, we could expect the breakeven line to move down and to the right.

VII. Using OpenConcept for Technology Assessment

A fundamental challenge faced by aircraft designers in industry is finding the right time to incorporate new technology onto an aircraft family. We learned in Section VI that a tipping point exists in the design space: an optimal conventional airplane will be as light as possible, but once batteries are economically favored, the best aircraft is as heavy as possible with batteries. This tendency makes retrofitting a hybrid or all-electric powertrain to an existing airframe infeasible, assuming the user wishes to fly similar mission ranges. Therefore, clean sheet designers must be able to predict at what point in time electrical component and battery technology will become economically favored for the chosen mission. OpenConcept can conduct the sort of low-cost, moderate-fidelity tradespace exploration required to answer this question.

The Section VI hybrid King Air airframe was heavy and had relatively high parasitic drag. To simulate improved airframe technology, the C_{D_0} was reduced from 0.022 to 0.018, and the structural weight factor reduced from 2.0 to 1.5 (a 33% structural weight reduction; for example, using carbon composites and reclaiming margin). We then ran an additional 252 MDO scenarios on the same range–versus–e_b grid, using the minimum cost optimization rules presented in Section VI. We also ran the full span of design ranges on the conventional twin turboprop model, using the same structural weight and drag reductions, to provide a fair comparison. The total time (including setup) to run the optimizations and analyze results was approximately 9 hours on a standard Windows laptop. Figure 8 illustrates the fuel burn, cost, weight, and energy.

We found that, as predicted, the lower-weight and lower-drag airplane favored electric propulsion at lower e_b across all ranges. The economic breakeven line moved down about 50 Wh/kg, nearly into the present-day feasibility zone for a 300 nmi mission (Figure 9). The line is also shallower, meaning that the effect of the weight and drag reduction is felt more strongly at longer ranges.

The published literature has contributed to industry understanding of the primary technical and performance drivers of electric flight. However, results from published studies are not general enough to tell a design team when to implement electric propulsion for their particular set of requirements. Using OpenConcept, designers can rapidly test their internal

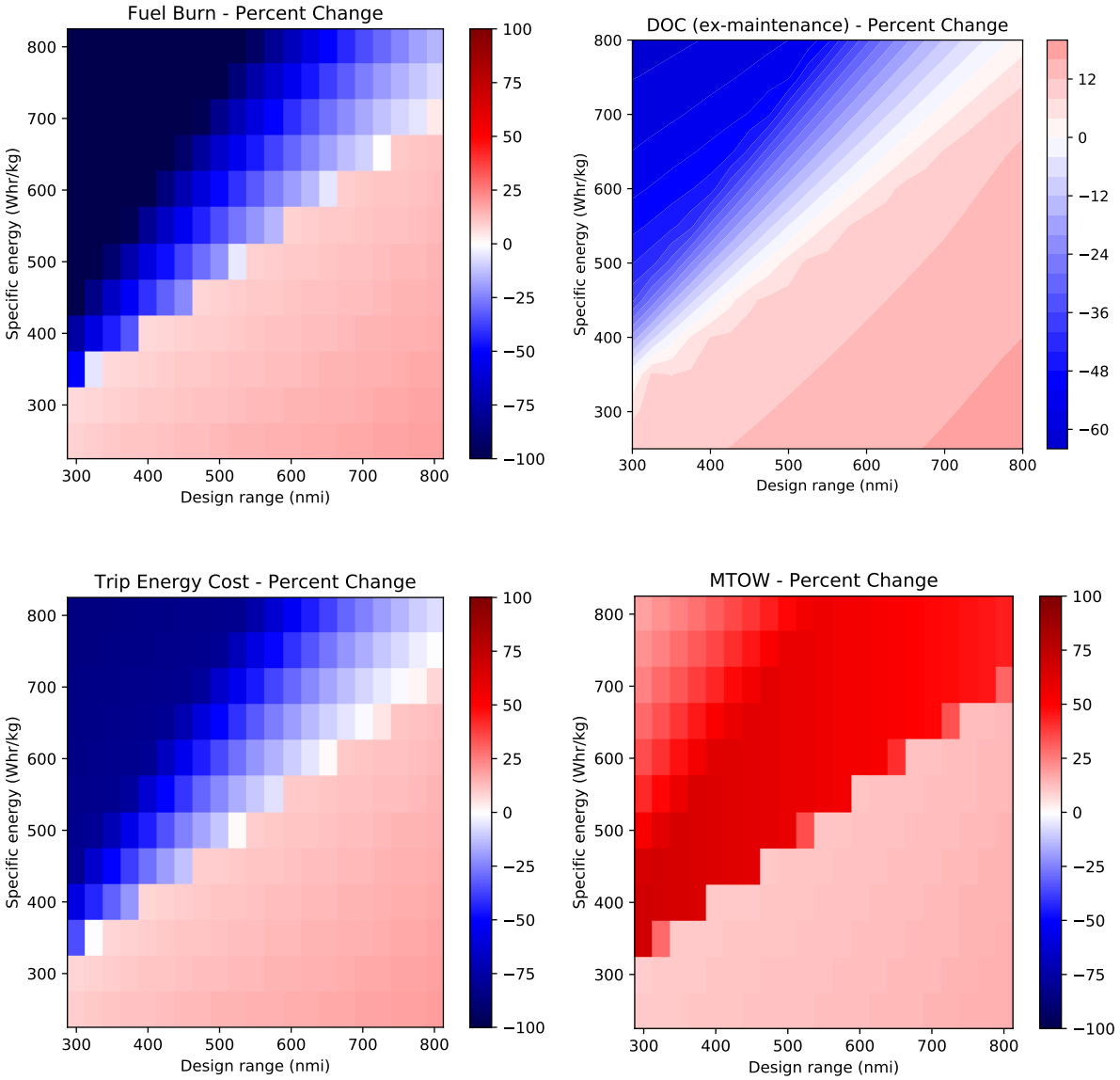

Fig. 7 Minimum Cost Hybrid vs Minimum Cost Conventional (MDO results)

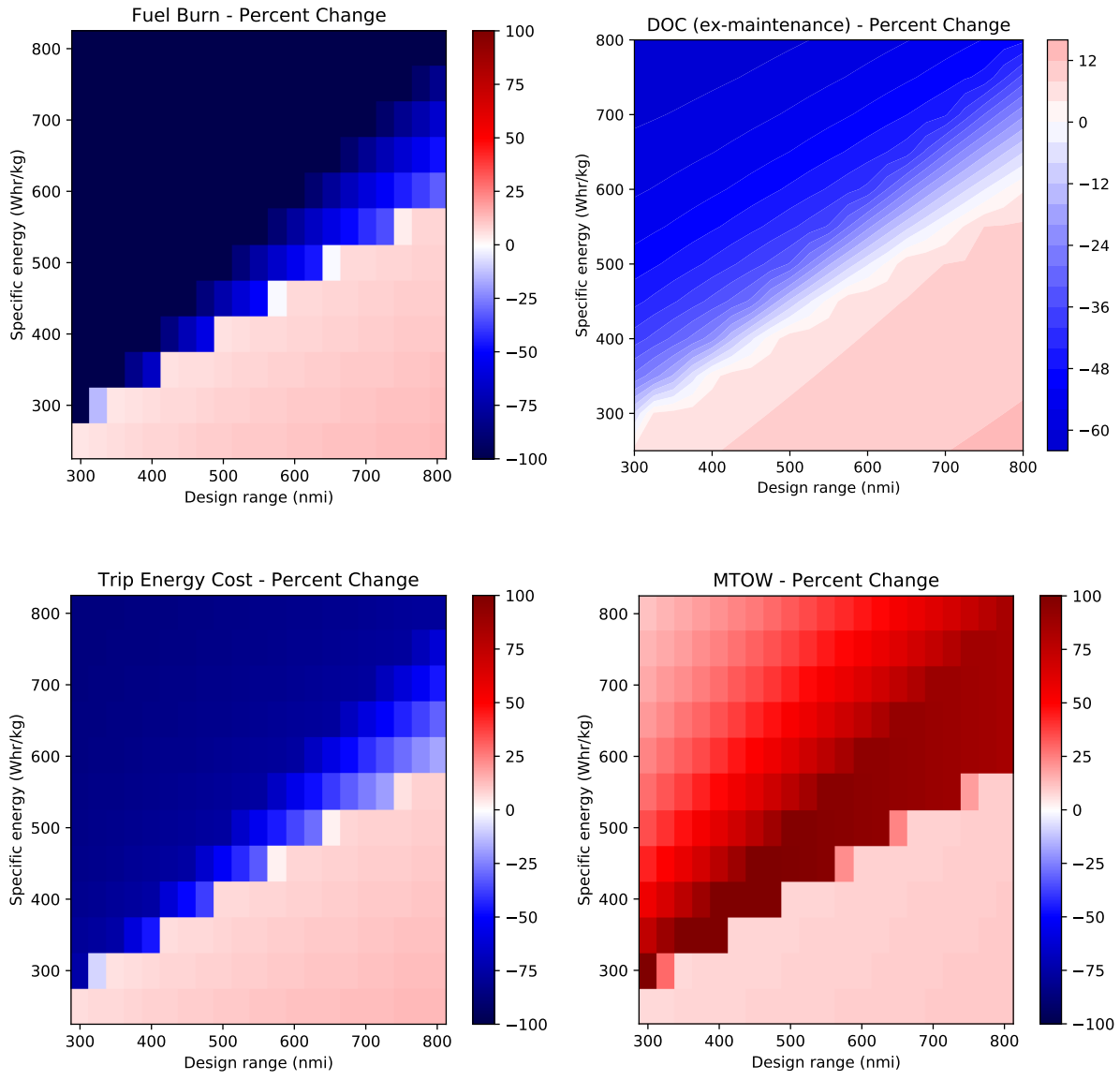

Fig. 8 Minimum Cost Hybrid vs Minimum Cost Conventional with reduced structural weight and drag (MDO results)

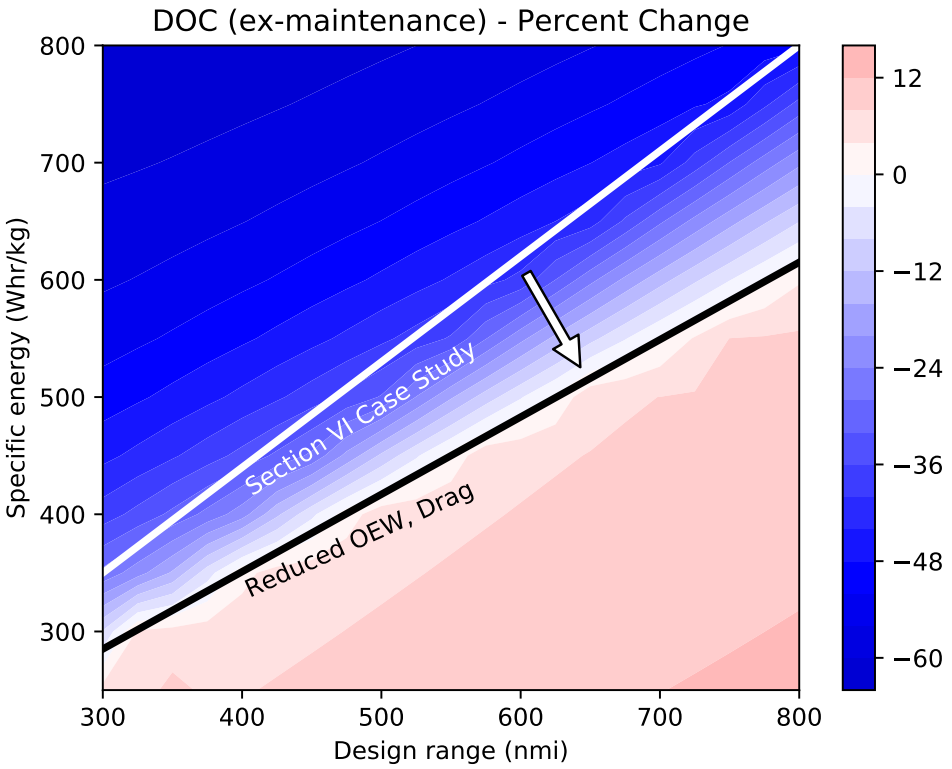

Fig. 9 Improved airframe technology makes electric propulsion economically feasible at lower specific energies

assumptions and generate large amounts of trade study data with modest setup time and computational resources. Similar studies could be conducted with respect to specific power or efficiency of individual electrical components, accounting for time-dependent heating and cooling constraints.

Table 4 Baseline analysis, component resizing, and MDO results (minimum fuel burn objective)

	TBM850 (Model)	TBM850 (Published)	King Air C90GT (Model)	King Air C90GT (Published)	Hybrid Conversion - Max Range	Hybrid Conversion 750	Hybrid Conversion 500	Hybrid Conversion 250	Hybrid MDO 1000	Hybrid MDO 750	Hybrid MDO 500	Hybrid MDO 250	King Air MDO 1000nmi	King Air MDO 500nmi
Optimization Rules	Analysis	Analysis	Analysis	Analysis	Comp Sizing	Comp Sizing	Comp Sizing	Comp Sizing	MDO	MDO	MDO	MDO	MDO	MDO
Specific Energy (Wh/kg)	–	–	–	–	750	750	500	250	1000	750	500	250	–	–
Design Range (nmi)	1250	1150+100	1000	894+100	761.6 (max)		500			500			1000	500
MTOW (lb)	7392	7392	10100	10100		10100			10156	12505	**12566**	8912.8	9367	7941
OEW (lb)	4756	4762	7177	7150	7433.9	7197	7328	7410	6755	7594	7967	6828.5	6827	6279
Max Fuel Wt (vol imit, lb)	2000	2000	2570	2570		2570			**1102**	**1102**	**1102**	**1102**	1540	**1102**
MLW (lb)	7000	7000	9600	9600		9600				9600			9600	
Rated TO SHP (each)	850	850	550	550	527.2	527.2	572.2	527.2	519.4	640.0	649.9	456.6	511.5	434.6
Turboshaft SHP (each)	850	850	550	550	1061.0	629.0	867.6	1018.2	–	–	641.1	940.0	511.5	434.6
Generator SHP	–	–	–	–	1029.2	610.6	841.5	987.6	–	–	630.4	907.9	–	–
Prop Diameter (ft)	7.58	7.58	7.50	7.50		7.50			**7.22**	**7.22**	**7.22**	**7.22**	**7.22**	**7.22**
PSFC (lb/hp/hr)	0.60		0.60			0.60				0.6			0.6	
Wing Ref Area (ft^2)	193.8	193.8	294.0	294.0		294.0			296.0	364.6	366.3	259.8	273.1	231.5
Wingspan (ft)	41.5	41.5	50.2	50.2		50.2			50.4	55.9	56.1	47.2	48.4	44.6
Aspect Ratio	8.95	8.95	8.58	8.58		8.58				8.58			8.58	
Flaps-Down $C_{L_{max}}$	1.70		1.52			1.52				1.52			1.52	
Oswald Efficiency	0.78		0.80			0.80				0.80			0.80	
C_{D0} at Cruise	0.0205		0.0220			0.0220				0.0220			0.0220	
C_{D0} at Takeoff	0.0300		0.0290			0.0290				0.0290			0.0290	
Takeoff Rotation Speed (kias)	89.6	90	89.8	90	89.8	89.8	89.8	89.8	89.8	89.8	89.8	89.8	89.8	89.8
Battery Wt (lb)	–	–	–	–	381.4	1397.9	1079.2	754.6	2400.8	3911.4	3077.6	330.3	–	–
Takeoff Battery %	–	–	–	–		100%				100%			–	–
Cruise Battery %	–	–	–	–	5.0%	43.7%	22.3%	8.6%	100.0%	100.0%	52.5%	3.6%	–	–
Design Payload (lb)	1000	1000	1000	1000		1000				1000			1000	
Cruise Speed (KIAS)	201	201	170	170		170				170			170	
Cruise Altitude (ft)	28000	28000	29000	29000		29000				29000			29000	
Climb Rate (ft/min)	1500		1500			1500				1500			1500	
Climb Speed (KIAS)	124		124			124				124			124	
Descent Speed (KIAS)	140		130			130				130			130	
BFL, SL, ISA+0 (ft)	2844	2838	4452	4519	**4452**	**4452**	**4452**	**4452**	**4452**	**4452**	**4452**	**4452**	**4452**	**4452**
BFL % Error	0.2%		-1.5%											
Cruise Fuel Flow (lb/hr)	414	415	468	612										
Cruise Fuel % Error	-0.3%		-23.5%											
Design Mission Fuel (lb)	1605.8		1663.8		1284.2	504.5	692.7	811.0	0.0	0.0	520.0	754.0	1540.3	663.4
Design Mission Fuel (lb/nmi)	1.285		1.664		1.686	1.009	1.385	1.622	0.000	0.000	1.040	1.508	1.540	1.327

Bold numbers indicate an active design variable bound or constraint

VIII. Conclusions

This paper examined unique features of the electric aircraft design problem and briefly surveyed the current state of electric aircraft modeling tools. We identified gaps in current capabilities. In particular, a need existed for an open-source mission analysis tool compatible with electric propulsion, including cost and thermal analysis. We introduced a new, open-source mission analysis and conceptual sizing tool—OpenConcept—written in Python and running atop of the OpenMDAO framework. OpenConcept's analytic gradients enable the use of Newton solvers and efficient gradient-based optimization. This enabled us to run hundreds of individual optimizations without high-performance computing hardware, and rapidly explore the electric propulsion tradespace for a twin series hybrid concept. More than 750 individual MDO cases across a wide range of battery specific energy levels and design ranges revealed discontinuities and tipping points in the design space. We demonstrated the ability to rigorously quantify the influence of operating economics on optimal fixed-wing hybrid electric aircraft design. While many published studies use fuel burn as an objective function, we find that this tendency may be overstating the economic benefit realizable through electric propulsion, especially at lower specific energies. Using operating cost as an objective function balances the weight gain due to electric propulsion with the fuel burn reduction in a more realistic way. Finally, we explore the effect of airframe technology on the conventional versus electric economic tipping point. A more efficient aerostructure substantially reduces the technological requirements necessary for electric propulsion to be economically favorable. The authors note that tipping points and trends in the design space for this airframe and architecture may not apply to other conceptual designs. Using OpenConcept, other researchers and designers may rigorously and rapidly examine the tradespace for each architecture, mission, and set of economic inputs.

Acknowledgements

The first author was supported by the National Science Foundation Graduate Research Fellowship Program under Grant DGE 1256260. Any opinions, findings, and conclusions or recommendations expressed in this material are those of the author(s) and do not necessarily reflect the views of the National Science Foundation. This work was also supported in part by the U.S. Air Force Research Laboratory (AFRL) under the Michigan-AFRL Collaborative Center in Aerospace Vehicle Design (CCAVD), with Dr. Richard Snyder as the task Technical Monitor. Justin Gray at NASA Glenn provided extensive advice and support for OpenMDAO.

References

[1] Moore, M. D., and Fredericks, B., "Misconceptions of Electric Aircraft and their Emerging Aviation Markets," *52nd Aerospace Sciences Meeting*, National Harbor, MD, 2014. doi:10.2514/6.2014-0535, URL http://arc.aiaa.org/doi/10.2514/6.2014-0535.

[2] Welstead, J., and Felder, J. L., "Conceptual Design of a Single-Aisle Turboelectric Commercial Transport with Fuselage Boundary Layer Ingestion," *54th AIAA Aerospace Sciences Meeting*, San Diego, CA, 2016. doi:10.2514/6.2016-1027, URL http://arc.aiaa.org/doi/10.2514/6.2016-1027.

[3] Borer, N. K., Patterson, M. D., Viken, J. K., Moore, M. D., Bevirt, J., Stoll, A. M., and Gibson, A. R., "Design and Performance of the NASA SCEPTOR Distributed Electric Propulsion Flight Demonstrator," *16th AIAA Aviation Technology, Integration, and Operations Conference*, Washington, DC, 2016. doi:10.2514/6.2016-3920, URL http://arc.aiaa.org/doi/10.2514/6.2016-3920.

[4] Gray, J., Mader, C. A., Kenway, G. K. W., and Martins, J. R. R. A., "Modeling Boundary Layer Ingestion Using a Coupled Aeropropulsive Analysis," *Journal of Aircraft*, Vol. 55, No. 3, 2018, pp. 1191–1199. doi:10.2514/1.C034601.

[5] Deere, K. A., Viken, J. K., Viken, S. A., Carter, M. B., Wiese, M. R., and Farr, N., "Computational Analysis of a Wing Designed for the X-57 Distributed Electric Propulsion Aircraft," *17th AIAA Aviation Technology, Integration, and Operations Conference*, Denver, CO, 2017. URL https://ntrs.nasa.gov/archive/nasa/casi.ntrs.nasa.gov/20170005883.pdf.

[6] Freeman, J., Osterkamp, P., Green, M. W., Gibson, A. R., and Schiltgen, B. T., "Challenges and opportunities for electric aircraft thermal management," *Aircraft Engineering and Aerospace Technology*, Vol. 86, No. 6, 2014, pp. 519–524. doi:10.1108/AEAT-04-2014-0042, URL http://www.emeraldinsight.com/doi/10.1108/AEAT-04-2014-0042.

[7] Hepperle, M., "Electric Flight – Potential and Limitations," Tech. rep., NATO, Braunschweig, 2012.

[8] Kenway, G. K. W., and Martins, J. R. R. A., "Multipoint High-Fidelity Aerostructural Optimization of a Transport Aircraft Configuration," *Journal of Aircraft*, Vol. 51, No. 1, 2014, pp. 144–160. doi:10.2514/1.C032150.

[9] Falck, R. D., Chin, J., Schnulo, S. L., Burt, J. M., and Gray, J. S., "Trajectory Optimization of Electric Aircraft Subject to Subsystem Thermal Constraints," *18th AIAA/ISSMO Multidisciplinary Analysis and Optimization Conference*, Denver, CO, 2017. doi:10.2514/6.2017-4002, URL https://arc.aiaa.org/doi/10.2514/6.2017-4002.

[10] Jansen, R. H., Bowman, C., and Jankovsky, A., "Sizing Power Components of an Electrically Driven Tail Cone Thruster and a Range Extender," *16th AIAA Aviation Technology, Integration, and Operations Conference*, Washington, DC, 2016. doi:10.2514/6.2016-3766.

[11] Perullo, C. A., and Mavris, D. N., "Assessment of Vehicle Performance Using Integrated NPSS Hybrid Electric Propulsion Models," *50th AIAA/ASME/SAE/ASEE Joint Propulsion Conference*, Cleveland, OH, 2014. doi:10.2514/6.2014-3489, URL http://dx.doi.org/10.2514/6.2014-3489.

[12] Gladin, J. C., Trawick, D., Perullo, C. A., Tai, J. C., and Mavris, D. N., "Modeling and Design of a Partially Electric Distributed Aircraft Propulsion System with GT-HEAT," *55th AIAA Aerospace Sciences Meeting*, Grapevine, TX, 2017, pp. 1–18. doi:10.2514/6.2017-1924, URL http://arc.aiaa.org/doi/10.2514/6.2017-1924.

[13] Welstead, J. R., Caldwell, D., Condotta, R., and Monroe, N., "An Overview of the Layered and Extensible Aircraft Performance System (LEAPS) Development," *2018 AIAA Aerospace Sciences Meeting*, Kissimmee, FL, 2018. doi:10.2514/6.2018-1754.

[14] Pornet, C., Gologan, C., Vratny, P. C., Seitz, A., Schmitz, O., Isikveren, A. T., and Hornung, M., "Methodology for Sizing and Performance Assessment of Hybrid Energy Aircraft," *Journal of Aircraft*, Vol. 52, No. 1, 2015, pp. 341–352. doi:10.2514/1.C032716, URL http://arc.aiaa.org/doi/10.2514/1.C032716.

[15] Brown, G. V., "Weights and Efficiencies of Electric Components of a Turboelectric Aircraft Propulsion System," *49th AIAA Aerospace Sciences Meeting*, Orlando, FL, 2011. doi:10.2514/6.2011-225, URL http://arc.aiaa.org/doi/10.2514/6.2011-225.

[16] Hwang, J. T., and Ning, A., "Large-scale multidisciplinary optimization of an electric aircraft for on-demand mobility," *2018 AIAA/ASCE/AHS/ASC Structures, Structural Dynamics, and Materials Conference*, Kissimmee, FL, 2018, pp. 1–18. doi:10.2514/6.2018-1384, URL https://arc.aiaa.org/doi/abs/10.2514/6.2018-1384.

[17] Bower, G., "Vahana Configuration Trade Study - Part II," , 2017. URL https://vahana.aero/vahana-configuration-trade-study-part-ii-1edcdac8ad93.

[18] Duffy, M. J., Wakayama, S. R., Hupp, R., Lacy, R., and Stauffer, M., "A Study in Reducing the Cost of Vertical Flight with Electric Propulsion," *17th AIAA Aviation Technology, Integration, and Operations Conference*, Denver, CO, 2017. doi:10.2514/6.2017-3442, URL https://arc.aiaa.org/doi/10.2514/6.2017-3442.

[19] Trawick, D., Perullo, C. A., Armstrong, M. J., Snyder, D., Tai, J. C., and Mavris, D. N., "Development and Application of GT-HEAT for the Electrically Variable Engine Design," *55th AIAA Aerospace Sciences Meeting*, Grapevine, TX, 2017. doi:10.2514/6.2017-1922, URL http://arc.aiaa.org/doi/10.2514/6.2017-1922.

[20] Antcliff, K. R., Guynn, M. D., Marien, T., Wells, D. P., Schneider, S. J., and Tong, M. T., "Mission Analysis and Aircraft Sizing of a Hybrid-Electric Regional Aircraft," *54th AIAA Aerospace Sciences Meeting*, San Diego, CA, 2016, pp. 1–18. doi:10.2514/6.2016-1028, URL http://arc.aiaa.org/doi/10.2514/6.2016-1028.

[21] Vratny, P. C., Gologan, C., Pornet, C., Isikveren, A. T., and Hornung, M., "Battery Pack Modeling Methods for Universally-Electric Aircraft," *4th CEAS Air and Space Conference*, Linkoping, Sweden, 2013.

[22] Wroblewski, G. E., and Ansell, P. J., "Mission Analysis and Emissions for Conventional and Hybrid-Electric Commercial Transport Aircraft," *2018 AIAA Aerospace Sciences Meeting*, Kissimmee, FL, 2018. doi:doi:10.2514/6.2018-2028, URL https://doi.org/10.2514/6.2018-2028.

[23] Cipolla, V., and Oliviero, F., "HyPSim : A Simulation Tool for Hybrid Aircraft Performance Analysis," *Variational Analysis and Aerospace Engineering*, 2016, pp. 95–116. doi:10.1007/978-3-319-45680-5.

[24] Capristan, F. M., and Welstead, J. R., "An Energy-Based Low-Order Approach for Mission Analysis of Air Vehicles in LEAPS," *2018 AIAA Aerospace Sciences Meeting*, Kissimmee, FL, 2018. doi:10.2514/6.2018-1755, URL https://arc.aiaa.org/doi/10.2514/6.2018-1755.

[25] Vegh, J. M., Alonso, J. J., Orra, T. H., and Ilario da Silva, C. R., "Flight Path and Wing Optimization of Lithium-Air Battery Powered Passenger Aircraft," *53rd AIAA Aerospace Sciences Meeting*, Kissimmee, FL, 2015. doi:10.2514/6.2015-1674, URL http://dx.doi.org/10.2514/6.2015-1674.

[26] Lents, C. E., Hardin, L. W., Rheaume, J., and Kohlman, L., "Parallel Hybrid Gas-Electric Geared Turbofan Engine Conceptual Design and Benefits Analysis," *52nd AIAA/SAE/ASEE Joint Propulsion Conference*, Salt Lake City, UT, 2016. doi:doi:10.2514/6.2016-4610, URL http://dx.doi.org/10.2514/6.2016-4610.

[27] Brelje, B. J., and Martins, J. R. R. A., "Electric, Hybrid, and Turboelectric Fixed-Wing Aircraft: A Review of Concepts, Models, and Design Approaches," *Progress in Aerospace Sciences*, 2018. (Submitted).

[28] Schiltgen, B. T., and Freeman, J., "Aeropropulsive Interaction and Thermal System Integration within the ECO-150: A Turboelectric Distributed Propulsion Airliner with Conventional Electric Machines," *16th AIAA Aviation Technology, Integration, and Operations Conference*, Washington, DC, 2016. doi:10.2514/6.2016-4064, URL http://arc.aiaa.org/doi/10.2514/6.2016-4064.

[29] Deere, K. A., Viken, S., Carter, M., Viken, J. K., Derlaga, J. M., and Stoll, A. M., "Comparison of High-Fidelity Computational Tools for Wing Design of a Distributed Electric Propulsion Aircraft," *35th AIAA Applied Aerodynamics Conference*, Denver, CO, 2017. doi:10.2514/6.2017-3925, URL https://arc.aiaa.org/doi/10.2514/6.2017-3925.

[30] Felder, J. L., Brown, G. V., Kim, H. D., and Chu, J., "Turboelectric Distributed Propulsion in a Hybrid Wing Body Aircraft," *20th International Symposium on Air Breathing Engines (ISABE)*, Gothenburg, Sweden, 2011.

[31] Isikveren, A. T., Kaiser, S., Pornet, C., and Vratny, P. C., "Pre-design strategies and sizing techniques for dual-energy aircraft," *Aircraft Engineering and Aerospace Technology*, Vol. 86, No. 6, 2014, pp. 525–542. doi:10.1108/AEAT-08-2014-0122, URL http://www.emeraldinsight.com/doi/10.1108/AEAT-08-2014-0122.

[32] Berton, J. J., and Haller, W. J., "A Noise and Emissions Assessment of the N3-X Transport," *52nd Aerospace Sciences Meeting*, National Harbor, MD, 2014. doi:10.2514/6.2014-0594, URL http://arc.aiaa.org/doi/10.2514/6.2014-0594.

[33] Green, M. W., Schiltgen, B. T., and Gibson, A. R., "Analysis of a Distributed Hybrid Propulsion System with Conventional Electric Machines," *48th AIAA/ASME/SAE/ASEE Joint Propulsion Conference*, Atlanta, GA, 2012. doi:10.2514/6.2012-3768.

[34] Armstrong, M. J., Ross, C. A. H., and Blackwelder, M. J., "Trade Studies for NASA N3-X Turboelectric Distributed Propulsion System Electrical Power System Architecture," *SAE International Journal of Aerospace*, Vol. 5, No. 2, 2012, pp. 325–335. doi:10.4271/2012-01-2163.

[35] Davies, K., Norman, P., Jones, C., Galloway, S., and Burt, G., "Modelling the Fault Behaviour of a Superconducting Turboelectric Distributed Propulsion Network Overview of Superconducting DC Networks," *SAE Technical Paper 2014-01-2142*, 2014. doi:10.4271/2014-01-2142.

[36] Kim, H. D., Felder, J. L., Tong, M. T., Berton, J. J., and Haller, W., "Turboelectric distributed propulsion benefits on the N3-X vehicle," *Aircraft Engineering and Aerospace Technology*, Vol. 86, No. 6, 2014, pp. 558–561. doi:10.1108/AEAT-04-2014-0037, URL http://www.emeraldinsight.com/doi/10.1108/AEAT-04-2014-0037.

[37] Schnulo, S. L., Chin, J., Smith, A. D., and Dubois, A., "Steady State Thermal Analyses of SCEPTOR X-57 Wingtip Propulsion," *17th AIAA Aviation Technology, Integration, and Operations Conference*, Denver, CO, 2017, pp. 1–14.

[38] Schiltgen, B., Green, M. W., Gibson, A. R., Hall, D. W., and Cummings, D. B., "Benefits and Concerns of Hybrid Electric Distributed Propulsion with Conventional Electric Machines," *48th AIAA/ASME/SAE/ASEE Joint Propulsion Conference*, Atlanta, GA, 2012. doi:doi:10.2514/6.2012-3769.

[39] Isikveren, A. T., Pornet, C., Vratny, P. C., and Schmidt, M., "Optimization of Commercial Aircraft Using Battery-Based Voltaic-Joule/Brayton Propulsion," *Journal of Aircraft*, Vol. 54, No. 1, 2017, pp. 246–261. doi:10.2514/1.C033885, URL http://arc.aiaa.org/doi/10.2514/1.C033885.

[40] Clarke, S., Redifer, M., Papathakis, K. V., Samuel, A., and Foster, T., "X-57 power and command system design," *2017 IEEE Transportation and Electrification Conference and Expo, ITEC 2017*, 2017, pp. 393–400. doi:10.1109/ITEC.2017.7993303, URL https://ntrs.nasa.gov/archive/nasa/casi.ntrs.nasa.gov/20170005579.pdf.

[41] Papathakis, K. V., Burkhardt, P. A., Ehmann, D. W., and Sessions, A. M., "Safety Considerations for Electric, Hybrid-Electric, and Turbo-Electric Distributed Propulsion Aircraft Testbeds," *53rd AIAA/SAE/ASEE Joint Propulsion Conference*, Atlanta, GA, 2017. doi:10.2514/6.2017-5032, URL https://arc.aiaa.org/doi/10.2514/6.2017-5032.

[42] Shaw, J. C., Norman, P., Galloway, S., and Burt, G., "A Method for the Evaluation of the Effectiveness of Turboelectric Distributed Propulsion Power System Architectures," *SAE International Journal of Aerospace*, Vol. 7, No. 1, 2014, pp. 35–43. doi:10.4271/2014-01-2120.

[43] Shaw, J. C., Fletcher, S., Norman, P., Galloway, S., and Burt, G., "Failure Analysis of a Turboelectric Distributed Propulsion Aircraft Electrical Network : A Case Study," *SAE Technical Paper 2015-01-2403*, 2015. doi:10.4271/2015-01-2403.

[44] Martins, J. R. R. A., and Lambe, A. B., "Multidisciplinary Design Optimization: A Survey of Architectures," *AIAA Journal*, Vol. 51, No. 9, 2013, pp. 2049–2075. doi:10.2514/1.J051895.

[45] Gray, J., Hearn, T., Moore, K., Hwang, J. T., Martins, J. R. R. A., and Ning, A., "Automatic Evaluation of Multidisciplinary Derivatives Using a Graph-Based Problem Formulation in OpenMDAO," *Proceedings of the 15th AIAA/ISSMO Multidisciplinary Analysis and Optimization Conference*, Atlanta, GA, 2014. doi:10.2514/6.2014-2042.

[46] Hwang, J. T., and Martins, J. R. R. A., "A computational architecture for coupling heterogeneous numerical models and computing coupled derivatives," *ACM Transactions on Mathematical Software*, 2018. (In press).

[47] Gray, J. S., Chin, J., Hearn, T., Hendricks, E., Lavelle, T., and Martins, J. R. R. A., "Chemical Equilibrium Analysis with Adjoint Derivatives for Propulsion Cycle Analysis," *Journal of Propulsion and Power*, Vol. 33, No. 5, 2017, pp. 1041–1052. doi:10.2514/1.B36215.

[48] Hearn, D. T., Hendricks, E., Chin, J., Gray, J. S., and Moore, D. K. T., "Optimization of Turbine Engine Cycle Analysis with Analytic Derivatives," *17th AIAA/ISSMO Multidisciplinary Analysis and Optimization Conference, part of AIAA Aviation 2016 (Washington, DC)*, 2016. doi:10.2514/6.2016-4297.

[49] Raymer, D. P., *Aircraft Design: A Conceptual Approach*, 5th ed., AIAA, 2012.

[50] Weisstein, E. W., "Simpson's Rule, from MathWorld–A Wolfram Web Resource," , 2003. URL `http://mathworld.wolfram.com/SimpsonsRule.html`.

[51] Hwang, J. T., Jasa, J. P., and Martins, J. R. R. A., "High-fidelity design-allocation optimization of a commercial aircraft maximizing airline profit," *Journal of Aircraft*, 2018. (Submitted).

[52] Roskam, J., *Airplane Design, Volumes 1-8*, Roskam Aviation and Engineering Corporation, 1989.

[53] Horne, T. A., "TBM 850 By the Numbers," *AOPA Pilot*, 2012.

[54] SOCATA-Daher, "Pilot's Information Manual - TBM 850 from S/N 434 to 999," , 2015.

[55] FrauTech, "Design Fridays: That's a big prop," , 2011. URL `https://frautech.wordpress.com/2011/01/28/design-fridays-thats-a-big-prop/`.

[56] Horne, T. A., "King Air C90GTi: More Power, More Panel," *AOPA Pilot*, 2008.